Supplement of Clim. Past, 21, 161–184, 2025
https://doi.org/10.5194/cp-21-161-2025-supplement
© Author(s) 2025. CC BY 4.0 License.

Climate of the Past
Open Access

Supplement of

Last-millennium volcanic forcing and climate response using SO_2 emissions

Lauren R. Marshall et al.

Correspondence to: Lauren R. Marshall (lrm27@st-andrews.ac.uk) and Anja Schmidt (anja.schmidt@dlr.de)

The copyright of individual parts of the supplement might differ from the article licence.

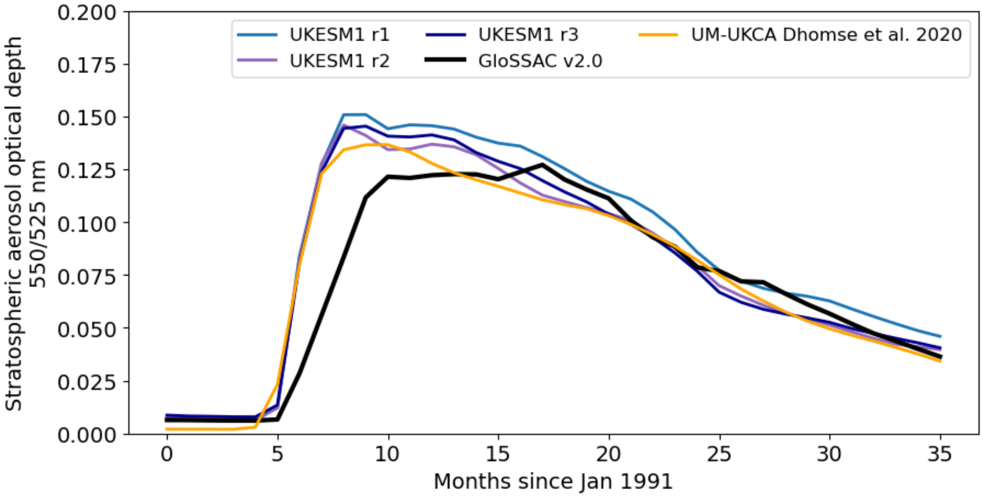

Figure S1. Global mean stratospheric aerosol optical depth following the 1991 Mt. Pinatubo eruption from our SO_2-driven UKESM1 simulations vs. UM-UKCA vn8.4 (Dhomse et al., 2020) and from observations (GloSSAC) (Thomason et al., 2018). In these simulations 10 Tg of SO_2 is emitted between 0 and 15°N at an altitude of 22-25 km in UKESM1 and 21-23 km in UM-UKCA. Simulated SAOD is at 550 nm; GloSSAC is at 525 nm.

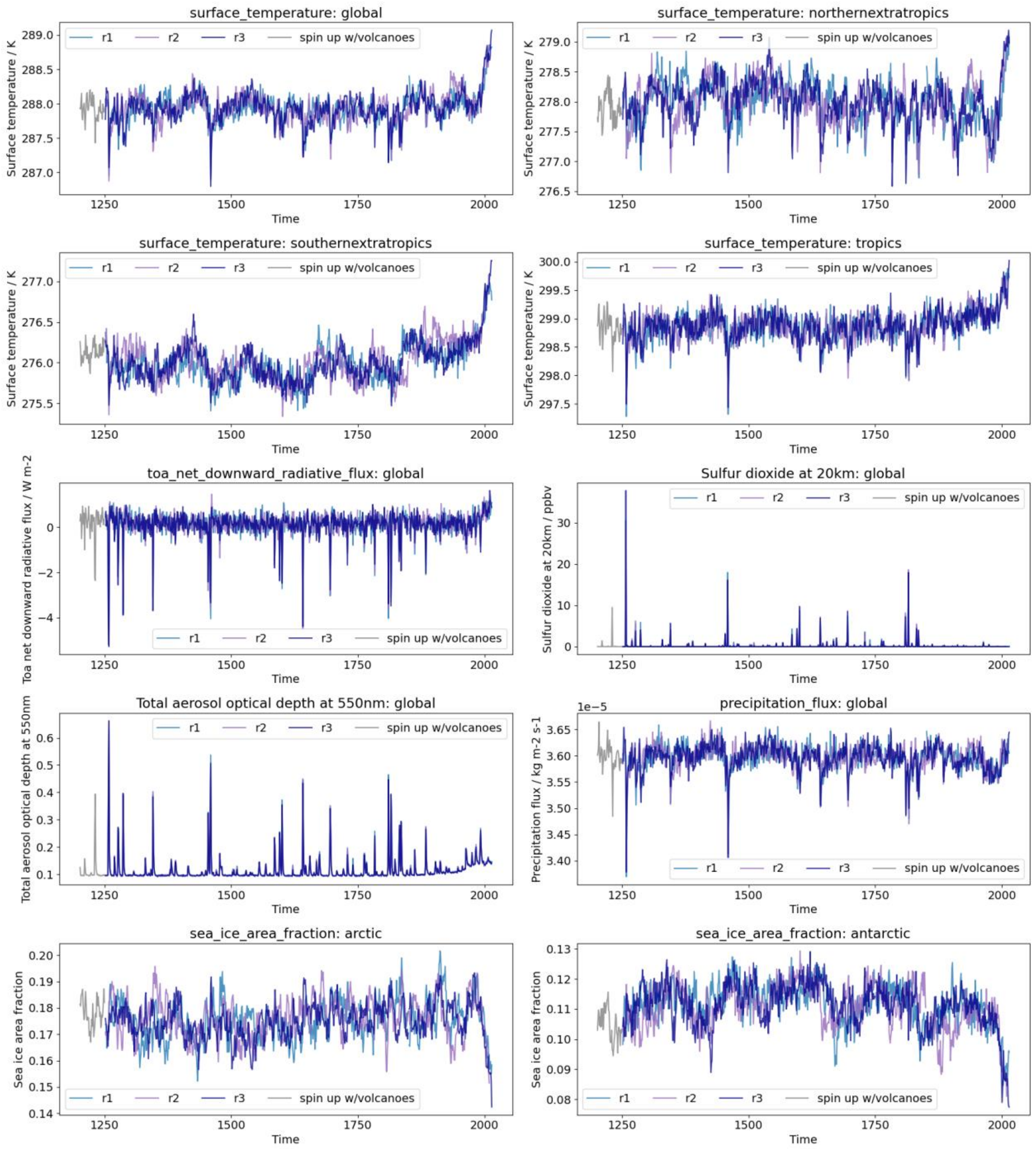

Figure S2. Annual mean atmospheric climate metrics. Due to restarts of the simulations, annual means shown here are missing for 1250, 1750 and 1850, as well as 1794, 1833 and 2010-2014 for r2, and 1429 and 1468 for r3.

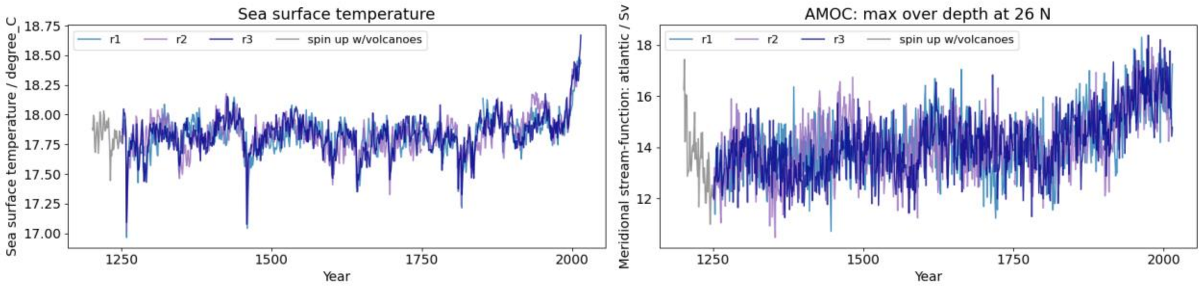

Figure S3. Global annual mean sea surface temperature and AMOC.

S1. SO_2 emissions implementation in MRI-ESM2

SO_2 emissions, eruption location and year are taken from eVolv2k (Toohey and Sigl, 2017), with unknown eruptions simulated on January 1st and at 0°E. The emission altitude is fixed at around 24 km. The model uses the MASINGAR mk-2r4c aerosol scheme; Model of Aerosol Species in the Global Atmosphere mark-2 revision 4-climate (Yukimoto et al., 2019).

S2. Extended model information for UKESM1

A summary of the forcing data and how it was implemented in our last millennium simulations is included in Table S1. The volcanic emissions dataset is included in Table S2, also shown in Figure S4. Three monthly mean files failed to archive: for surface temperature, July 1696 from ensemble member 2 and Feb 1285 from ensemble member 3, and for SAOD, March 1284 from ensemble member 3. These datapoints are consequently ignored in any analysis. The closest eruptions are in 1276 (therefore not affected by the 1284 and 1285 missing files) and 1693 and 1695 but these eruptions are not a focus of our study and do not affect our results.

Table S1. Forcing data and its implementation in UKESM1.

Forcing	Details
GHG concentrations	GHG mmr specified for use in radiation scheme. GHG vmr used by the chemistry scheme (Meinshausen et al., 2017).
Solar	PMIP4 forcing data (14C SATIRE) processed by SOCRATES radiation code as described in Jungclaus et al. (2017).
Volcanic forcing interactive	SO_2 emissions provided by Toohey and Sigl (2017) with two updates: 1. For unidentified eruptions, the season was randomly assigned to either January, April, July or October. The eruptions included are listed in Table S2. 2. For Laki, we used daily emissions (Schmidt et al., 2010). In UKESM the grid boxes meet at the equator and therefore all tropical unidentified eruptions had the SO_2 emission injected into the grid box at 0-1.25° N. Emissions were spread between 18 and 20 km.
Aerosol & chemistry emissions	Transient emissions from 1750 onwards following Hoesly et al. (2018), constant 1750 emissions from 1250-1749.
Land-use change (crop/pasture)	Crops and pasture fractions set following the CMIP6 forcing (Hurtt et al., 2020). Other vegetation fractions determined by a dynamical vegetation scheme (TRIFFID).
Nitrogen deposition	1850 climatology used.
Ozone	Interactive chemistry. No change to ozone from changes to incoming UV.

Table S2. Volcanic emissions dataset. Eruptions that are simulated in different seasons to the EVA(2k) dataset are highlighted in grey.

Event number	**Day**	**Month**	**Year**	**SO_2 mass (Tg SO_2)**	**Latitude (°N)**	**Longitude (°E)**	**Volcano name**
1	1	1	1890	0.8	-45	140	unidentified
2	10	6	1886	1.48	-38	176.5	Okataina
3	27	8	1883	18.68	-6	105.4	Krakatau
4	1	4	1875	1.34	65	-16.7	Askja
5	8	1	1873	2.34	64.4	-17.3	Grimsvoetn
6	1	12	1861	9.06	0.3	127.4	Makian
7	25	9	1856	2.52	42.1	140.7	Hokkaido_Komagatake
8	22	4	1853	2.72	42.5	140.8	Toya
9	1	4	1846	1.94	45	140	unidentified
10	20	1	1835	18.96	13	-87.6	Cosigueina
11	1	7	1831	25.96	19.5	121.9	Babuyan_Claro*
12	8	10	1822	4.04	-7.3	108.1	Galunggung
13	1	1	1821	1.1	-45	140	unidentified
14	10	4	1815	56.16	-8	118	Tambora
15	1	10	1809	38.52	0	140	unidentified
16	1	7	1797	1.48	45	140	unidentified
17	1	10	1796	1.38	45	140	unidentified
18	1	4	1786	1.66	45	140	unidentified
19	15	6	1783	41.62	64.4	-17.3	Laki**
20	1	10	1770	1.4	45	140	unidentified
21	5	4	1766	5.04	64	-19.7	Hekla
22	1	4	1762	9.64	0	140	unidentified
23	17	10	1755	2.36	63.6	-19.1	Katla
24	19	8	1739	6.88	42.7	141.4	Shikotsu
25	1	1	1729	9.64	45	140	unidentified
26	11	5	1721	1.62	63.6	-19.1	Katla
27	1	7	1720	1.44	45	140	unidentified
28	16	12	1707	2.16	35.4	138.7	Fujisan
29	1	4	1695	31.48	0	140	unidentified
30	1	10	1693	5.64	0	140	unidentified
31	20	5	1673	9.34	1.4	127.5	Gamkonora
32	23	9	1667	6.96	42.7	141.4	Shikotsu
33	1	7	1662	1.52	-45	140	unidentified
34	1	7	1654	7.44	0	140	unidentified
35	1	4	1646	4.84	45	140	unidentified
36	26	12	1640	37.36	6.1	124.9	Parker
37	1	7	1637	2.6	45	140	unidentified
38	1	1	1621	3.26	-45	140	unidentified
39	17	2	1600	37.9	-16.6	-70.85	Huaynaputina
40	1	3	1595	17.74	4.9	-75.3	Nevado_del_Ruiz
41	1	10	1590	0.98	-45	140	unidentified
42	10	4	1585	17.02	19.5	-103.62	Colima
43	1	1	1576	0.8	-45	140	unidentified
44	1	7	1567	5.02	45	140	unidentified
45	1	7	1554	4.82	0	140	unidentified
46	1	4	1541	1.9	-45	140	unidentified
47	1	1	1537	1.7	45	140	unidentified
48	1	7	1528	2.16	45	140	unidentified
49	1	10	1512	0.42	-45	140	unidentified
50	25	7	1510	4.6	64	-19.7	Hekla
51	1	1	1505	1.74	-45	140	unidentified
52	1	4	1502	2	45	140	unidentified
53	1	7	1480	3.32	45	140	unidentified

54	1	10	1478	2.36	-45	140	unidentified
55	1	2	1477	10.24	64.6	-17.51	Bardarbunga
56	1	1	1470	2.78	45	140	unidentified
57	1	7	1463	1.22	45	140	unidentified
58	1	7	1458	65.96	0	140	unidentified
59	1	10	1453	19.94	0	140	unidentified
60	1	10	1448	1.48	-45	140	unidentified
61	1	4	1441	1.6	45	140	unidentified
62	1	4	1414	3.8	0	140	unidentified
63	1	4	1389	6.52	0	140	unidentified
64	1	1	1381	4.92	0	140	unidentified
65	1	7	1378	1.86	-45	140	unidentified
66	1	1	1345	30.22	0	140	unidentified
67	1	1	1341	2.34	45	140	unidentified
68	1	7	1336	1.34	-45	140	unidentified
69	1	10	1329	7.38	45	140	unidentified
70	1	10	1306	1.44	-45	140	unidentified
71	1	1	1286	30.12	0	140	unidentified
72	1	4	1276	23.06	0	140	unidentified
73	1	1	1269	6.34	-45	140	unidentified
74	1	1	1260	2.1	45	140	unidentified
75	1	7	1257	118.84	-8.4	116.47	Samalas
76	1	4	1236	0.76	-45	140	unidentified
77	1	7	1230	47.56	0	140	unidentified
78	1	7	1222	1.74	45	140	unidentified
79	1	1	1210	6.58	45	140	unidentified
80	1	10	1200	6.58	45	140	unidentified
81	1	4	1191	17.06	0	140	unidentified
82	1	4	1182	20.1	45	140	unidentified
83	1	7	1180	0.58	-45	140	unidentified
84	1	1	1171	36.1	0	140	unidentified
85	1	7	1137	2.12	45	140	unidentified
86	1	10	1127	7.36	0	140	unidentified
87	1	4	1118	0.6	-45	140	unidentified
88	1	10	1115	1.56	45	140	unidentified
89	1	10	1108	38.32	0	140	unidentified
90	1	4	1092	0.46	-45	140	unidentified
91	1	1	1067	1.34	45	140	unidentified
92	1	4	1064	1.88	45	140	unidentified
93	1	1	1057	1.66	45	140	unidentified
94	1	4	1039	4.14	-45	140	unidentified
95	1	7	1028	15.56	0	140	unidentified
96	1	7	1020	3.94	45	140	unidentified
97	1	4	1011	3.22	45	140	unidentified
98	1	7	1003	9.96	0	140	unidentified
99	1	1	998	2.06	45	140	unidentified
100	1	1	990	0.42	-45	140	unidentified
101	1	10	982	3.08	45	140	unidentified
102	1	4	976	12.48	0	140	unidentified
103	1	4	970	2.2	45	140	unidentified
104	1	7	960	3.04	-45	140	unidentified
105	1	7	958	1.36	45	140	unidentified
106	1	10	953	1.76	45	140	unidentified
107	1	11	946	3.44	42	128.1	Changbaishan
108	1	4	939	32.46	63.6	-19.1	Eldgja
109	1	10	929	8.12	0	140	unidentified
110	1	4	916	12.16	0	140	unidentified
111	1	4	908	1.48	45	140	unidentified

112	1	7	904	7.7	45	140	unidentified
113	1	7	900	11.12	0	140	unidentified
114	1	10	880	2.56	45	140	unidentified
115	1	11	879	6.1	64.6	-17.51	Bardarbunga
116	1	4	876	3.84	45	140	unidentified
117	1	1	869	1.02	-45	140	unidentified
118	1	4	859	7.98	0	140	unidentified
119	1	1	853	4.96	61.4	-141.75	Churchill
120	1	10	853	2.44	-45	140	unidentified
121	1	4	841	1.94	45	140	unidentified
122	1	7	835	1.6	45	140	unidentified
123	1	7	827	0.5	-45	140	unidentified
124	1	10	822	7.86	45	140	unidentified
125	1	11	819	2.7	-45	140	unidentified
126	1	4	817	18.68	45	140	unidentified
127	1	1	800	4.96	45	140	unidentified

*This eruption may be falsely attributed (Garrison et al., 2018). **Daily emissions used to represent Laki in UKESM1 and CESM2(WACCM6ma)

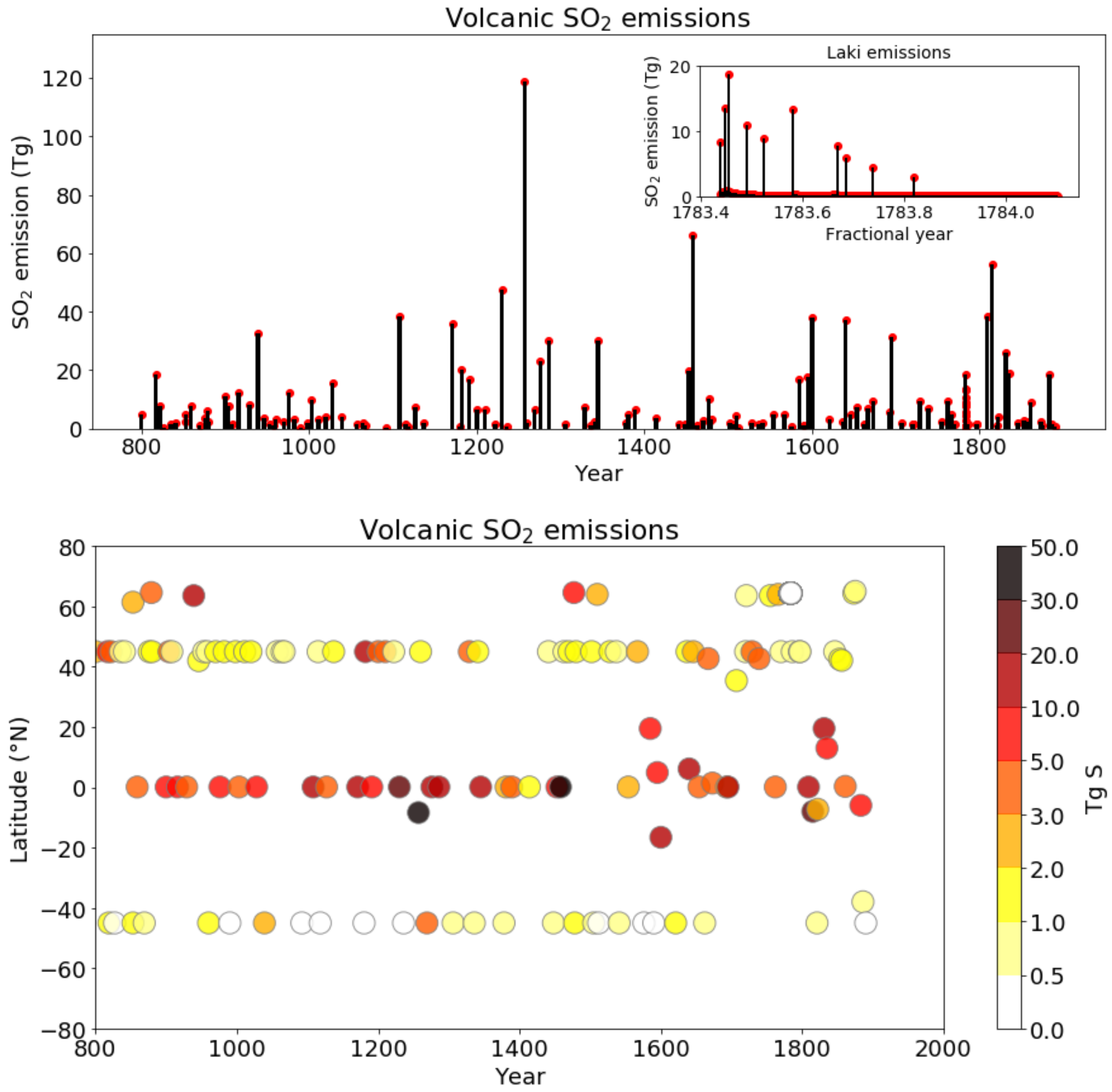

Figure S4. Volcanic emissions dataset. Top: total SO_2 emission including high-resolution emissions for Laki. Bottom: Latitude of emission.

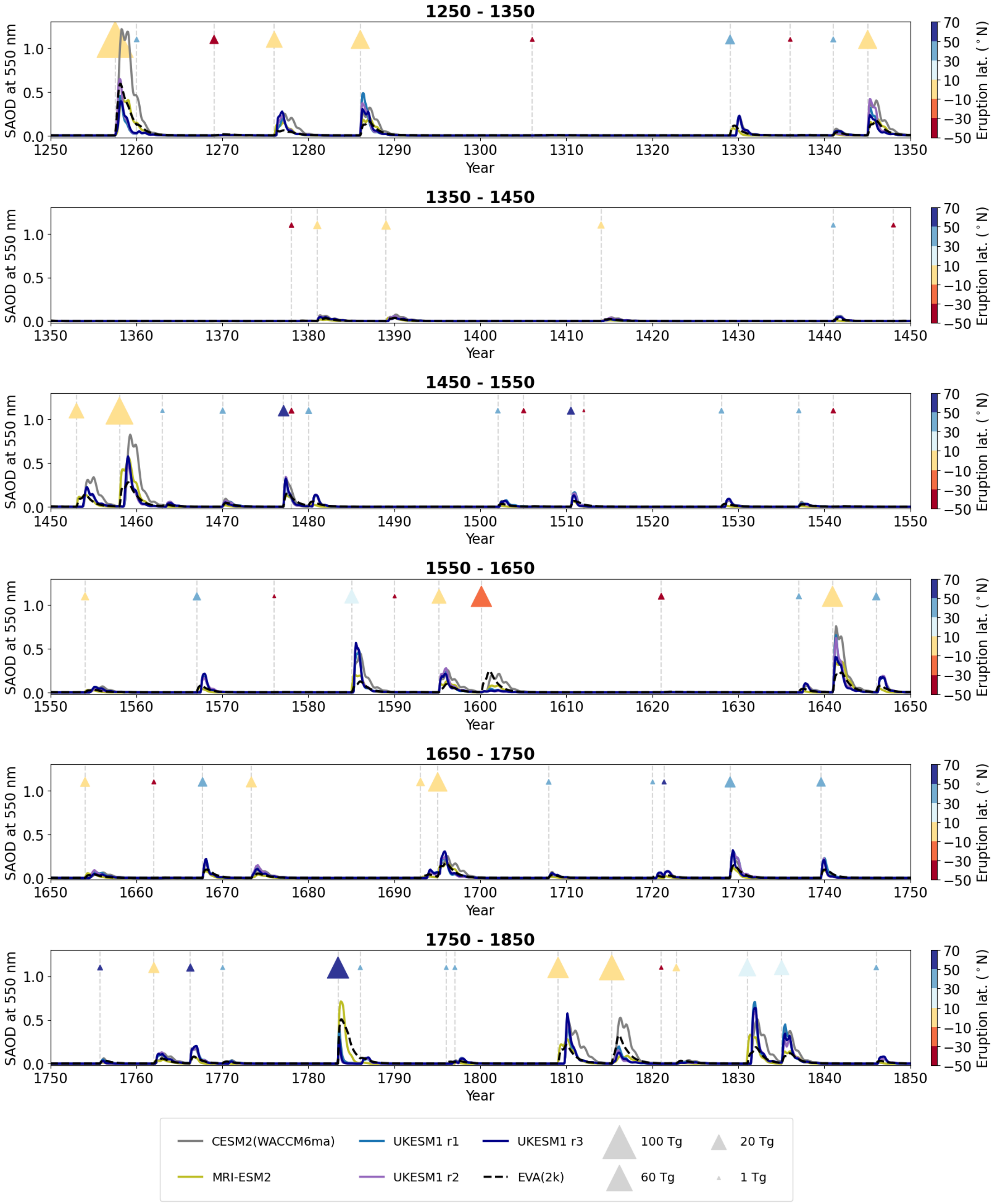

Figure S5. As Figure 1, but for the Northern Hemisphere SAOD averaged between 20°N and 90°N.

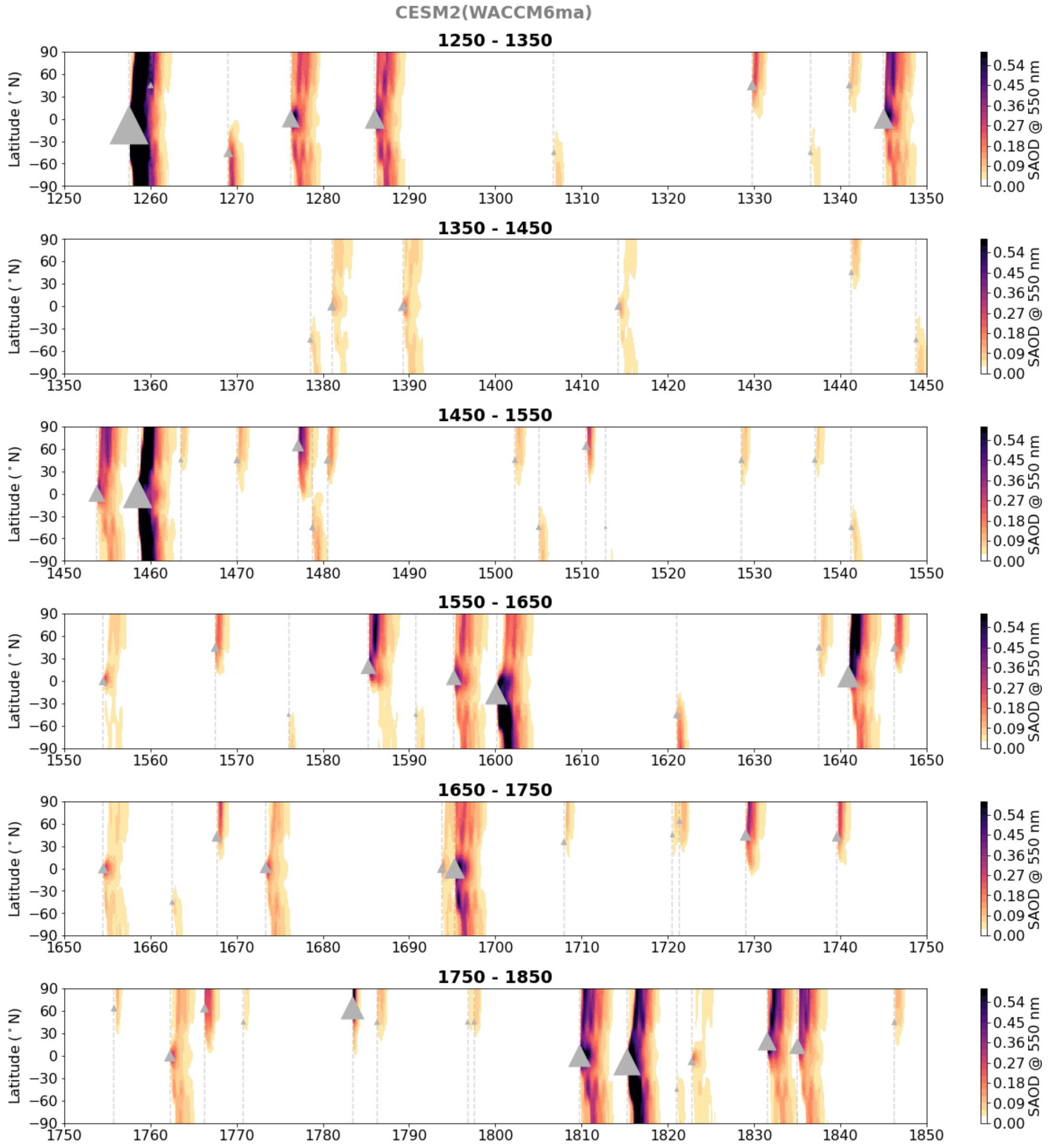

Figure S6. Zonal mean SAOD in CESM2(WACCM6ma) in 100-year chunks. Eruptions are marked by grey triangles and the size indicates the magnitude of the SO_2 emission, ranging from 0.4 Tg (for the 1512 Unidentified eruption) to 118 Tg (for the 1257 eruption of Samalas).

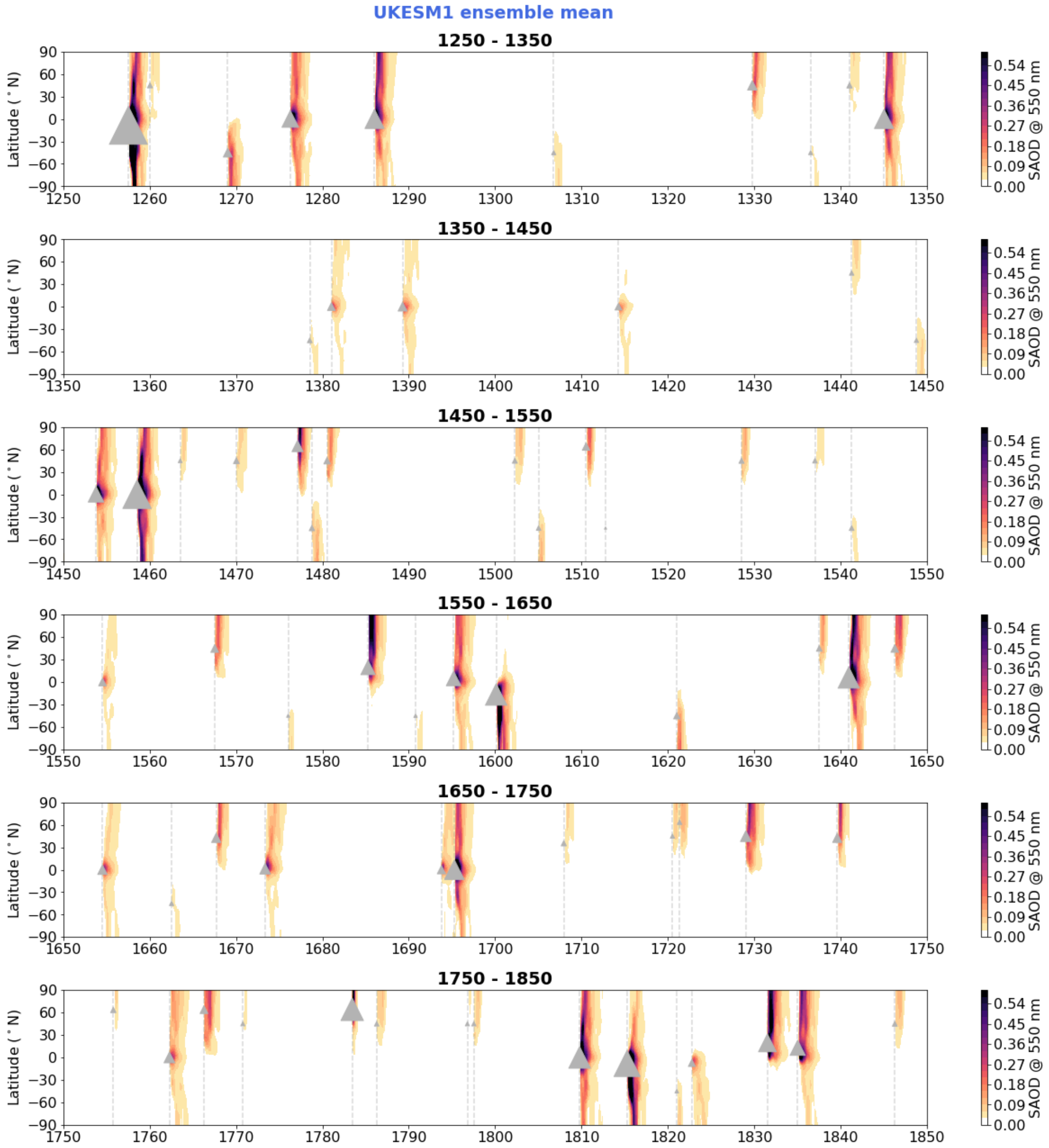

Figure S7. As Figure S6 but for the UKESM1 ensemble mean.

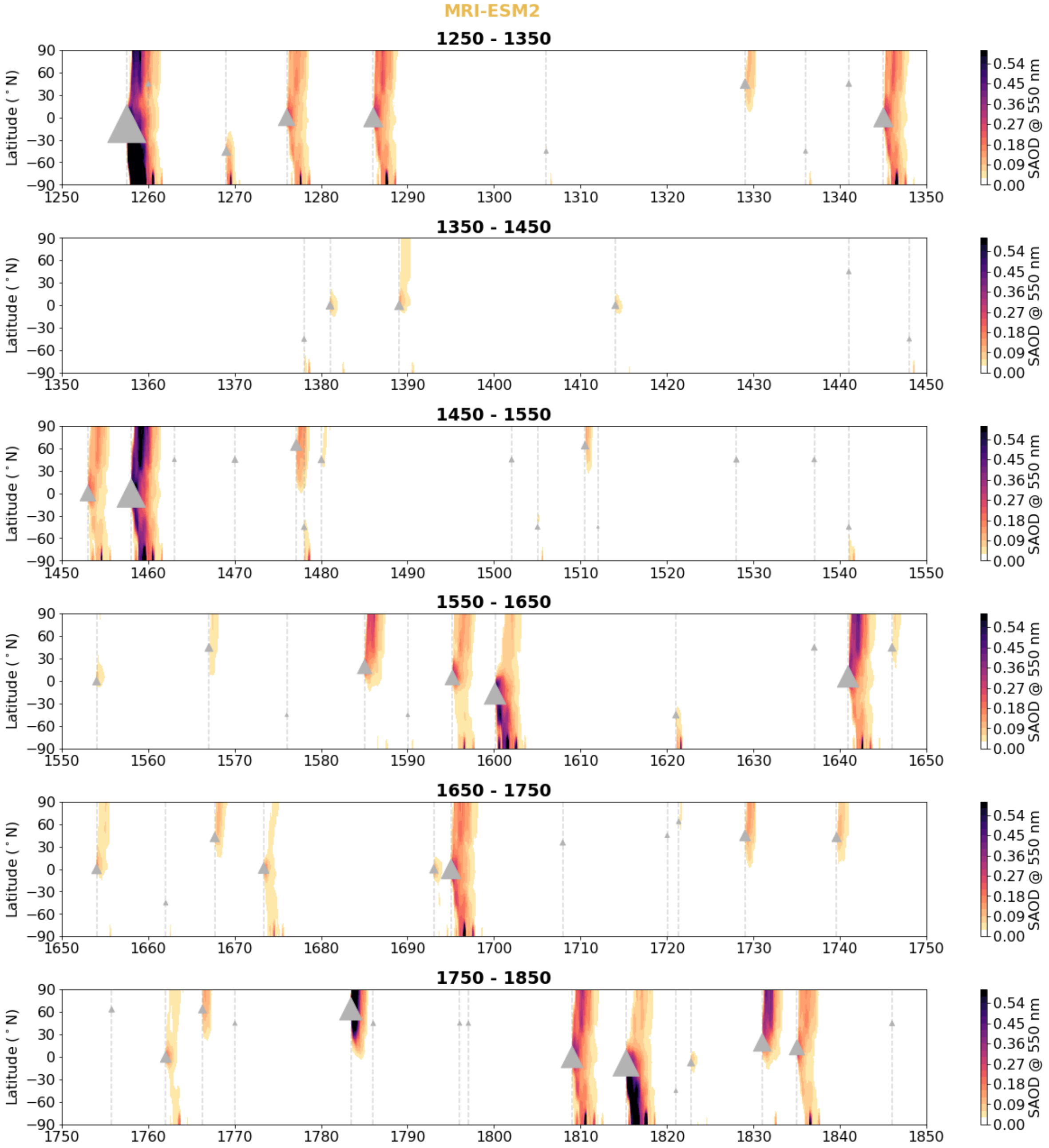

Figure S8. As Figure S6 but for MRI-ESM2.

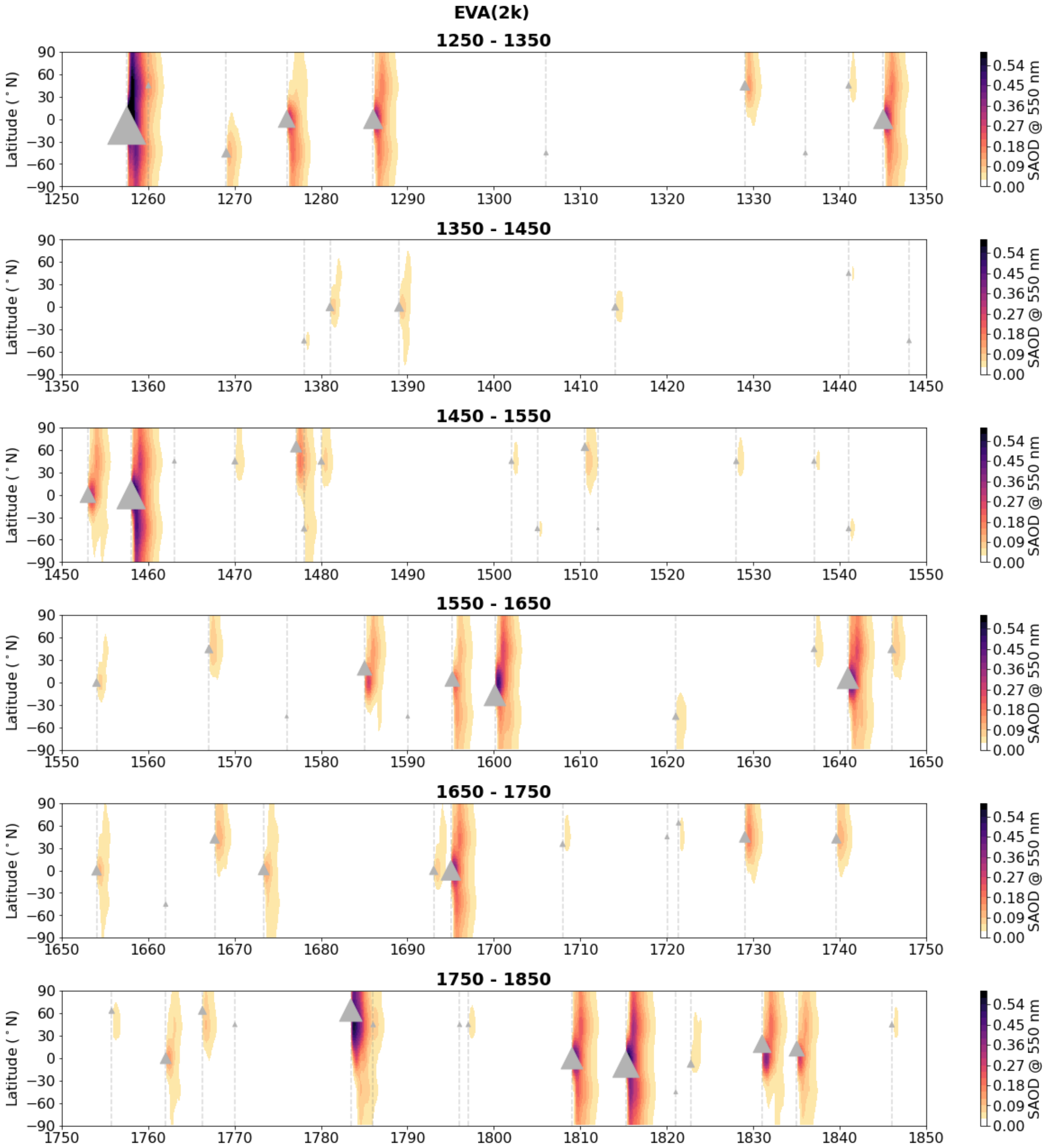

Figure S9. As Figure S6 but for EVA(2k).

Table S3. Volcanic events included in superposed epoch analysis with anomaly reference period

Event	**Anomaly reference period**	**Double event**
1257	5 years prior	N
1276	5 years prior	N
1286	5 years prior	N
1345	1336-1340 (eruption in 1341)	N
1453	5 years prior	1458 removed
1458	1448-1452 (eruption in 1453)	1463 removed
1477	1465-1469 (eruption in 1470)	1480 removed
1585	5 years prior	N
1595	5 years prior	1600 removed
1600	1590-1594 (eruption in 1595)	N
1640	1632-1636 (eruption in 1637)	1646 removed
1695	1688-1692 (eruption in 1693)	N
1783	5 years prior	1786 removed
1809	5 years prior	1815 removed
1815	1804-1808 (eruption in 1809)	1822 removed
1831	5 years prior	1835 removed
1835	1826-1830 (eruption in 1831)	N

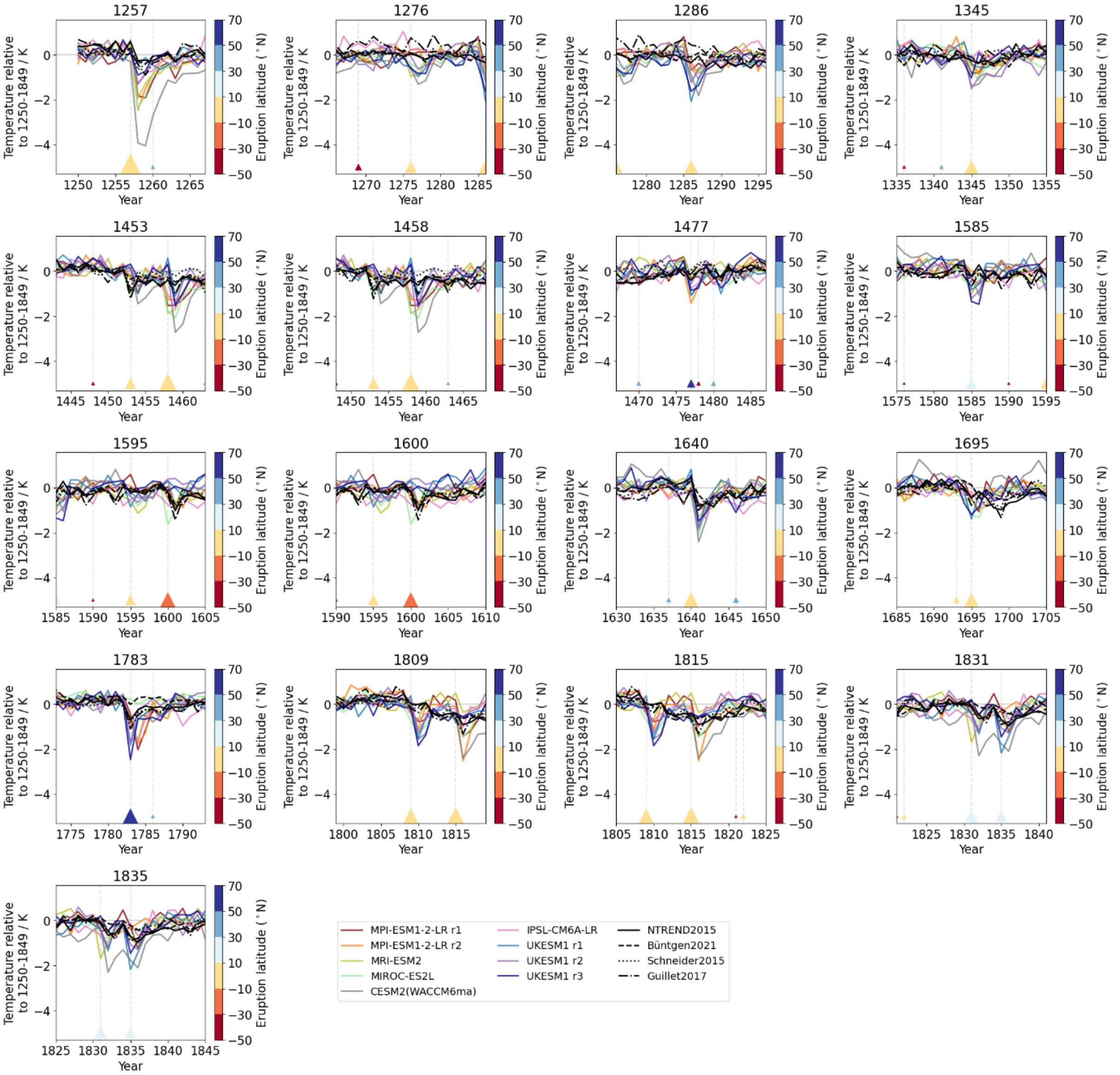

Figure S10. NH summer land surface air temperature anomalies (as in Figure 4) for the 17 large-magnitude eruptions (>10 Tg).

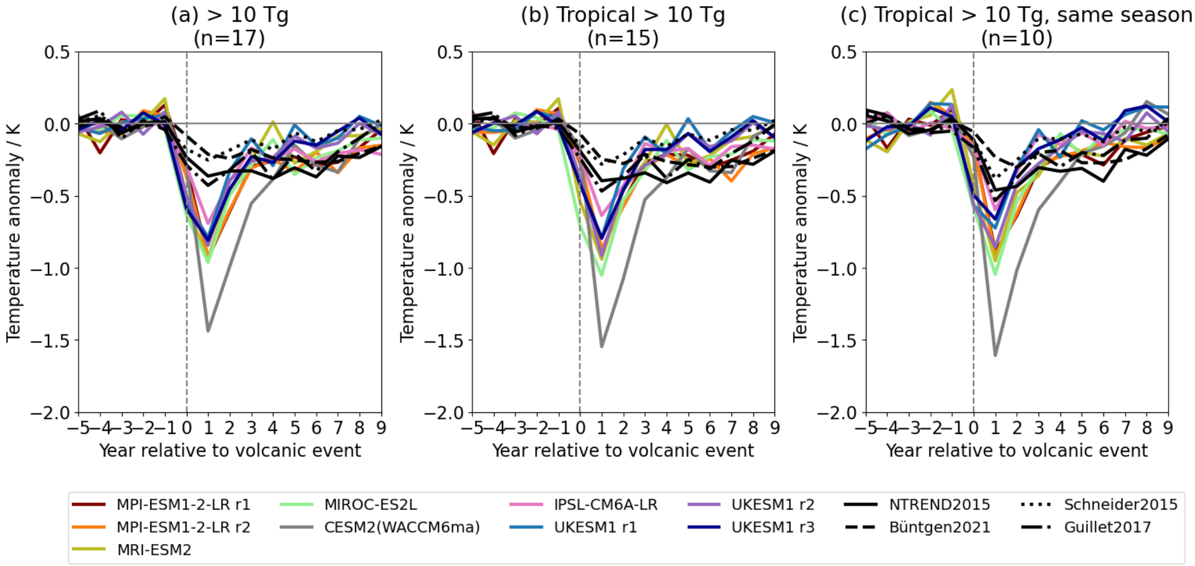

Figure S11. SEA as in Figure 3 but with all anomalies with reference to the 5-years prior to each eruption and double event data not removed.

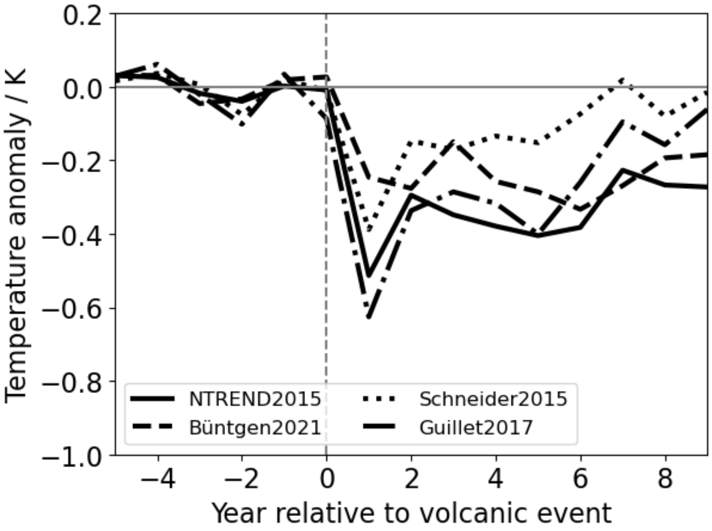

Figure S12. SEA for optimized dates in the four tree-ring reconstructions. Volcanic years used = 1257, 1277, 1287, 1344, 1458, 1584, 1600, 1640, 1694, 1808, 1815, 1831, 1835.

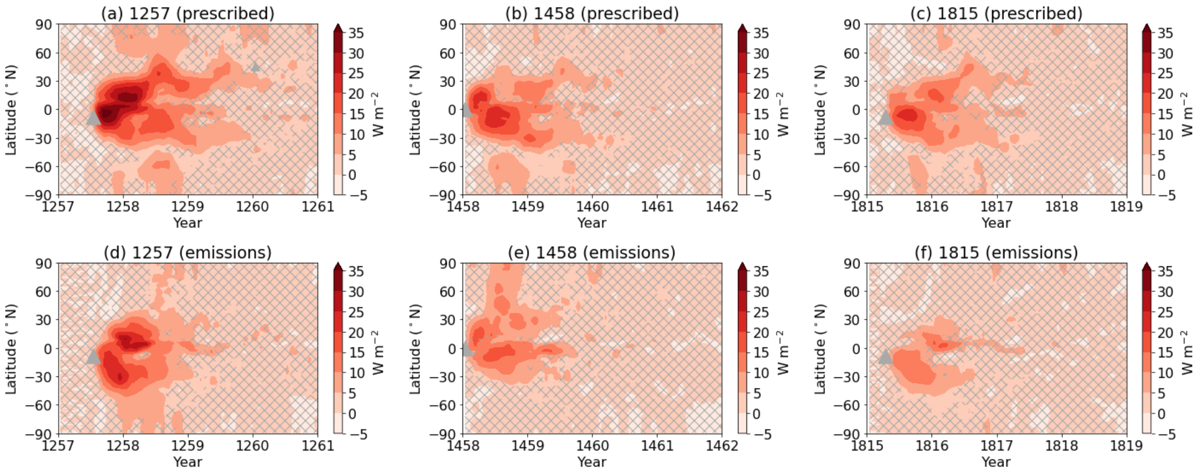

Figure S13. Zonal mean longwave anomalies.

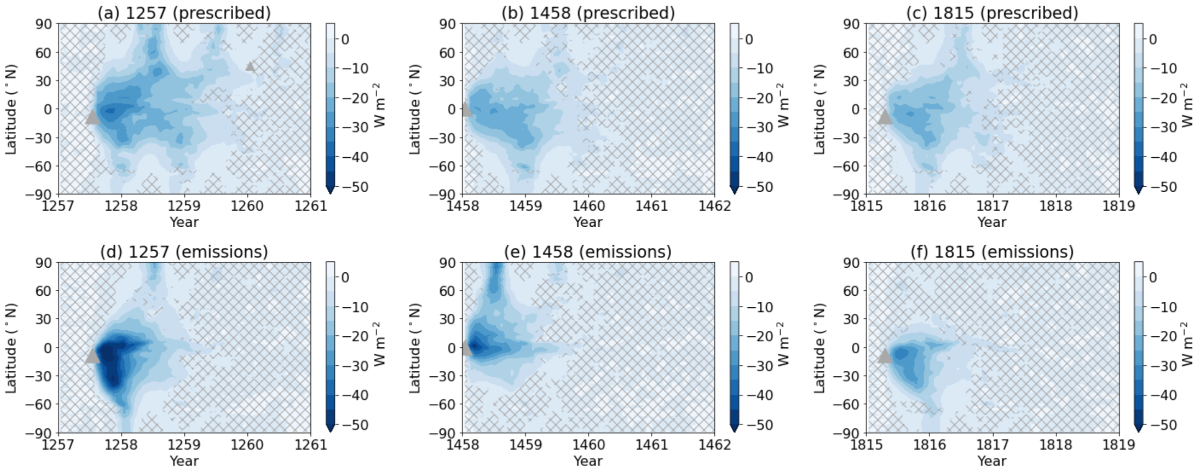

Figure S14. Zonal mean shortwave anomalies.

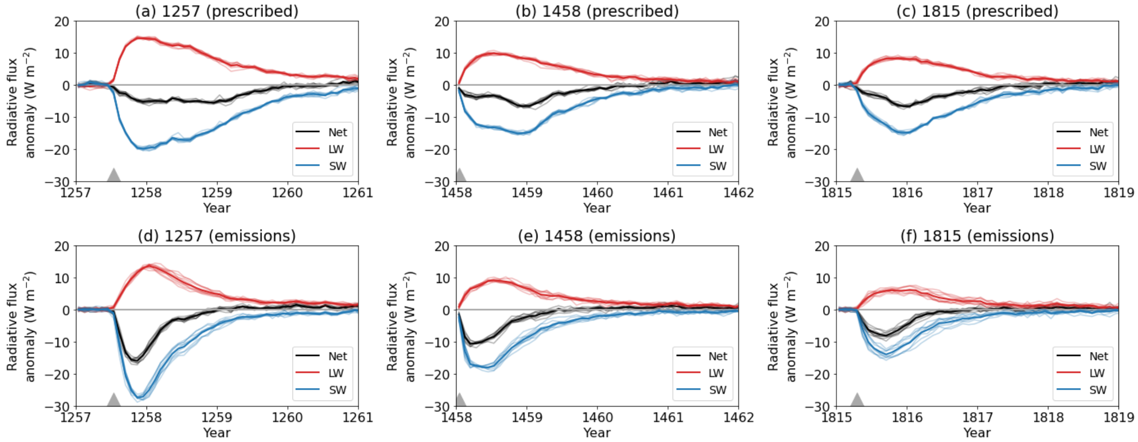

Figure S15. Global mean radiative flux anomalies. Longwave (LW) fluxes shown in red, shortwave (SW) in blue, and net in black. The ensemble mean values are shown in the thicker line.

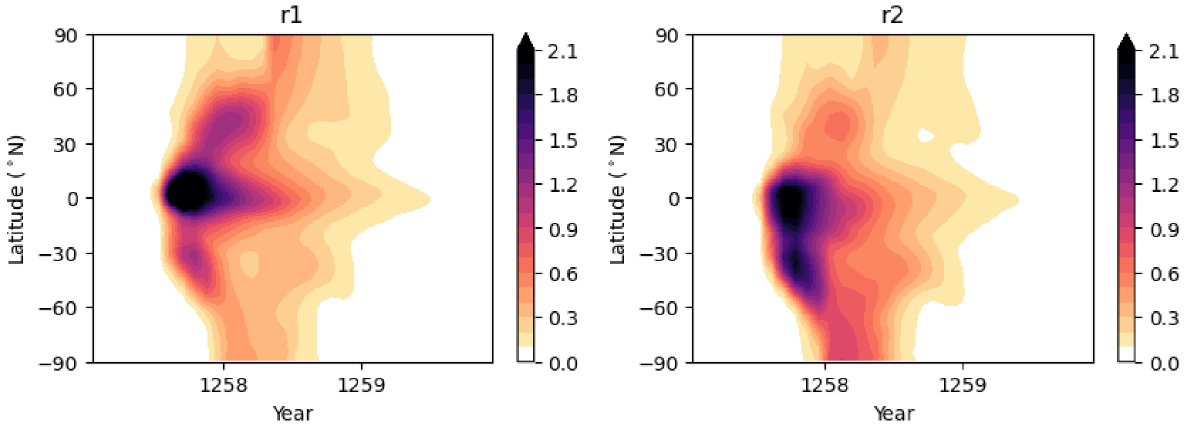

Figure S16. Zonal mean SAOD for 1257 Samalas simulated at 0°N for two ensemble members.

References

Dhomse, S. S., Mann, G. W., Antuña Marrero, J. C., Shallcross, S. E., Chipperfield, M. P., Carslaw, K. S., Marshall, L., Abraham, N. L., and Johnson, C. E.: Evaluating the simulated radiative forcings, aerosol properties, and stratospheric warmings from the 1963 Mt Agung, 1982 El Chichón, and 1991 Mt Pinatubo volcanic aerosol clouds, Atmos. Chem. Phys., 20, 13627-13654, 10.5194/acp-20-13627-2020, 2020.

Garrison, C. S., Kilburn, C. R. J., and Edwards, S. J.: The 1831 eruption of Babuyan Claro that never happened: has the source of one of the largest volcanic climate forcing events of the nineteenth century been misattributed?, Journal of Applied Volcanology, 7, 8, 10.1186/s13617-018-0078-9, 2018.

Hoesly, R. M., Smith, S. J., Feng, L., Klimont, Z., Janssens-Maenhout, G., Pitkanen, T., Seibert, J. J., Vu, L., Andres, R. J., Bolt, R. M., Bond, T. C., Dawidowski, L., Kholod, N., Kurokawa, J. I., Li, M., Liu, L., Lu, Z., Moura, M. C. P., O'Rourke, P. R., and Zhang, Q.: Historical (1750–2014) anthropogenic emissions of reactive gases and aerosols from the Community Emissions Data System (CEDS), Geosci. Model Dev., 11, 369-408, 10.5194/gmd-11-369-2018, 2018.

Hurtt, G. C., Chini, L., Sahajpal, R., Frolking, S., Bodirsky, B. L., Calvin, K., Doelman, J. C., Fisk, J., Fujimori, S., Klein Goldewijk, K., Hasegawa, T., Havlik, P., Heinimann, A., Humpenöder, F., Jungclaus, J., Kaplan, J. O., Kennedy, J., Krisztin, T., Lawrence, D., Lawrence, P., Ma, L., Mertz, O., Pongratz, J., Popp, A., Poulter, B., Riahi, K., Shevliakova, E., Stehfest, E., Thornton, P., Tubiello, F. N., van Vuuren, D. P., and Zhang, X.: Harmonization of global land use change and management for the period 850–2100 (LUH2) for CMIP6, Geosci. Model Dev., 13, 5425-5464, 10.5194/gmd-13-5425-2020, 2020.

Jungclaus, J. H., Bard, E., Baroni, M., Braconnot, P., Cao, J., Chini, L. P., Egorova, T., Evans, M., González-Rouco, J. F., Goosse, H., Hurtt, G. C., Joos, F., Kaplan, J. O., Khodri, M., Klein Goldewijk, K., Krivova, N., LeGrande, A. N., Lorenz, S. J., Luterbacher, J., Man, W., Maycock, A. C., Meinshausen, M., Moberg, A., Muscheler, R., Nehrbass-Ahles, C., Otto-Bliesner, B. I., Phipps, S. J., Pongratz, J., Rozanov, E., Schmidt, G. A., Schmidt, H., Schmutz, W., Schurer, A., Shapiro, A. I., Sigl, M., Smerdon, J. E., Solanki, S. K., Timmreck, C., Toohey, M., Usoskin, I. G., Wagner, S., Wu, C. J., Yeo, K. L., Zanchettin, D., Zhang, Q., and Zorita, E.: The PMIP4 contribution to CMIP6 – Part 3: The last millennium, scientific objective, and experimental design for the PMIP4 past1000 simulations, Geosci. Model Dev., 10, 4005-4033, 10.5194/gmd-10-4005-2017, 2017.

Meinshausen, M., Vogel, E., Nauels, A., Lorbacher, K., Meinshausen, N., Etheridge, D. M., Fraser, P. J., Montzka, S. A., Rayner, P. J., Trudinger, C. M., Krummel, P. B., Beyerle, U., Canadell, J. G., Daniel, J. S., Enting, I. G., Law, R. M., Lunder, C. R., O'Doherty, S., Prinn, R. G., Reimann, S., Rubino, M., Velders, G. J. M., Vollmer, M. K., Wang, R. H. J., and Weiss, R.: Historical greenhouse gas concentrations for climate modelling (CMIP6), Geosci. Model Dev., 10, 2057-2116, 10.5194/gmd-10-2057-2017, 2017.

Schmidt, A., Carslaw, K. S., Mann, G. W., Wilson, M., Breider, T. J., Pickering, S. J., and Thordarson, T.: The impact of the 1783–1784 AD Laki eruption on global aerosol formation processes and cloud condensation nuclei, Atmos. Chem. Phys., 10, 6025-6041, 10.5194/acp-10-6025-2010, 2010.

Thomason, L. W., Ernest, N., Millán, L., Rieger, L., Bourassa, A., Vernier, J. P., Manney, G., Luo, B., Arfeuille, F., and Peter, T.: A global space-based stratospheric aerosol climatology: 1979–2016, Earth Syst. Sci. Data, 10, 469-492, 10.5194/essd-10-469-2018, 2018.

Toohey, M. and Sigl, M.: Volcanic stratospheric sulfur injections and aerosol optical depth from 500 BCE to 1900 CE, Earth Syst. Sci. Data, 9, 809-831, 10.5194/essd-9-809-2017, 2017.

Yukimoto, S., Kawai, H., Koshiro, T., Oshima, N., Yoshida, K., Urakawa, S., Tsujino, H., Deushi, M., Tanaka, T., Hosaka, M., Yabu, S., Yoshimura, H., Shindo, E., Mizuta, R., Obata, A., Adachi, Y., and Ishii, M.: The Meteorological Research Institute Earth System Model Version 2.0, MRI-ESM2.0: Description and Basic Evaluation of the Physical Component, Journal of the Meteorological Society of Japan. Ser. II, 97, 931-965, 10.2151/jmsj.2019-051, 2019.